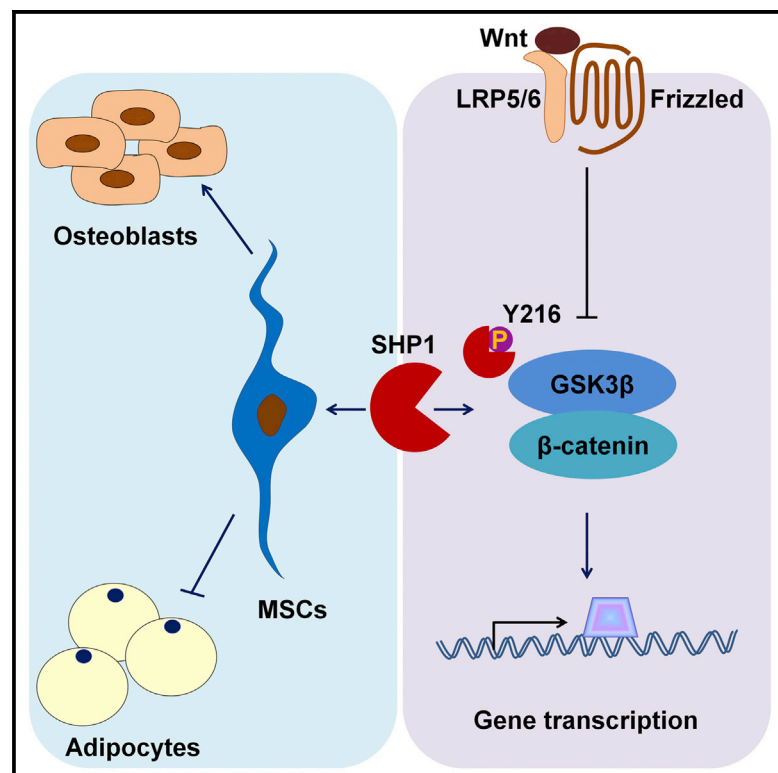


SHP1 Regulates Bone Mass by Directing Mesenchymal Stem Cell Differentiation

Graphical Abstract



Authors

Menghui Jiang, Chunxing Zheng, Peishun Shou, ..., Weifen Xie, Ying Wang, Yufang Shi

Correspondence

yingwang@sibs.ac.cn (Y.W.), yufangshi@sibs.ac.cn (Y.S.)

In Brief

The fate of differentiating MSCs influences the development of obesity and osteoporosis. Jiang et al. report that SHP1 controls MSC differentiation through binding to GSK3β and suppressing its kinase activity. These findings reveal a role for SHP1 in controlling bone and fat mass by modulating MSC differentiation.

Highlights

- SHP1 influences osteogenic differentiation of MSCs
- SHP1 deficiency leads to severe osteoporosis
- SHP1 affects osteogenesis through dephosphorylating GSK3β

SHP1 Regulates Bone Mass by Directing Mesenchymal Stem Cell Differentiation

Menghui Jiang,¹ Chunxing Zheng,¹ Peishun Shou,¹ Na Li,¹ Gang Cao,¹ Qing Chen,¹ Chunliang Xu,¹ Liming Du,¹ Qian Yang,¹ Jianchang Cao,¹ Yanyan Han,¹ Fengying Li,¹ Wei Cao,¹ Feng Liu,¹ Arnold B. Rabson,³ Arthur I. Roberts,³ Weifen Xie,⁴ Ying Wang,^{1,*} and Yufang Shi^{1,2,3,*}

¹Key Laboratory of Stem Cell Biology, Institute of Health Sciences, Shanghai Jiao Tong University School of Medicine and Shanghai Institutes for Biological Sciences, Chinese Academy of Sciences, Shanghai 200031, China

²The Third Affiliated Hospital of Soochow University, Institutes for Translational Medicine, Soochow University, Suzhou 215006, China

³Rutgers Cancer Institute of New Jersey, New Brunswick, NJ 80903, USA

⁴Changzheng Hospital, the Second Military Medical University, Shanghai 200433, China

*Correspondence: yingwang@sibs.ac.cn (Y.W.), yufangshi@sibs.ac.cn (Y.S.)

<http://dx.doi.org/10.1016/j.celrep.2016.06.035>

SUMMARY

Osteoblasts and adipocytes are derived from a common precursor, mesenchymal stem cells (MSCs). Alterations in the normal fate of differentiating MSCs are involved in the development of obesity and osteoporosis. Here, we report that *viable motheaten* (*me^v*) mice, which are deficient in the SH2-domain-containing phosphatase-1 (SHP1), develop osteoporosis spontaneously. Consistently, MSCs from *me^v/me^v* mice exhibit significantly reduced osteogenic potential and greatly increased adipogenic potential. When MSCs were transplanted into nude mice, SHP1-deficient MSCs resulted in diminished bone formation compared with wild-type MSCs. SHP1 was found to bind to GSK3 β and suppress its kinase activity by dephosphorylating pY216, thus resulting in β -catenin stabilization. Mice, in which SHP1 was deleted in MSCs using SHP1^{fl/fl} Dermo1-cre, displayed significantly decreased bone mass and increased adipose tissue. Taken together, these results suggest a possible role for SHP1 in controlling tissue homeostasis through modulation of MSC differentiation via Wnt signaling regulation.

INTRODUCTION

Mesenchymal stem cells (MSCs) are multipotent and can differentiate into one of several distinct cell lineages under appropriate conditions, including cartilage-forming chondrocytes (Wu et al., 2013), bone-forming osteoblasts (Pittenger et al., 1999), and fat-forming adipocytes, as well as myoblasts, fibroblasts, skeletal muscle cells (Moroni and Fornasari, 2013), and neurogenic lineages (Chamberlain et al., 2007). In addition, several studies have demonstrated an inverse relationship between adipogenesis and osteogenesis (James et al., 2012; Pei and Tontonoz, 2004). An imbalance between adipogenesis and osteogenesis can lead to various metabolic disorders, including osteoporosis, osteopetrosis, and obesity (Uccelli et al., 2008).

MSC differentiation is influenced by several key lineage-specific transcription factors: C/EBP α , C/EBP β , and C/EBP δ (CCAAT/enhancer-binding proteins) (Darlington et al., 1998), as well as PPAR γ (peroxisome proliferation-activated receptor γ) (Zhang et al., 2010), are critical for adipogenesis, while Runx2 (Runt-related transcription factor 2) (Neve et al., 2011) is vital for osteoblast differentiation. Indeed, several intrinsic signaling pathways that regulate the expression of lineage-specific transcription factors have been shown to guide MSC differentiation toward either the osteoblast or adipocyte lineages, including Wnt/ β -catenin signaling. Activation of Wnt/ β -catenin signaling in MSCs favors osteogenesis at the expense of adipogenesis by modulating the availability of cell-type-specific transcription factors (Bennett et al., 2005). Conversely, disruption of Wnt/ β -catenin signaling leads to spontaneous adipogenesis by MSCs and pre-adipocytes. Wnt/ β -catenin signaling regulates the fate of MSCs by suppressing adipocyte transcription factors, by stimulating the production of osteoblast transcription factors, or by both mechanisms (Bennett et al., 2005).

The Src homology protein, SHP1 is predominantly expressed in hematopoietic cells. SHP1 is traditionally considered to negatively regulate hematopoietic and immune cell function (Shultz et al., 1997). However, its role in stem cells and some progenitor cells has only recently been described. SHP1 has been shown to participate in modulating the stemness of mouse embryonic stem cells (ESCs) (Cha et al., 2010) and to be involved in neuronal differentiation (Mizuno et al., 1997). SHP1 activity is completely absent in the murine *motheaten* mutation (*me/me*), whereas the *viable motheaten* mutation (*me^v/me^v*) retains about 25% of SHP1 activity. Both of these mutants exhibit classic symptoms of osteoporosis (Green and Shultz, 1975), including significantly lower bone marrow density and mineral content in the femur, compared to wild-type (WT) mice, although the mechanism is not clear.

It has been suggested that osteoporosis results from imbalanced differentiation of MSCs into either osteoblasts or adipocytes. In the present study, we investigated whether osteoporosis observed in SHP1-deficient mice is due to a cell-autonomous function of SHP1 in MSC differentiation. We find that SHP1 promotes osteogenesis and inhibits adipogenesis in MSCs by modulating Wnt/ β -catenin signaling. Importantly, we

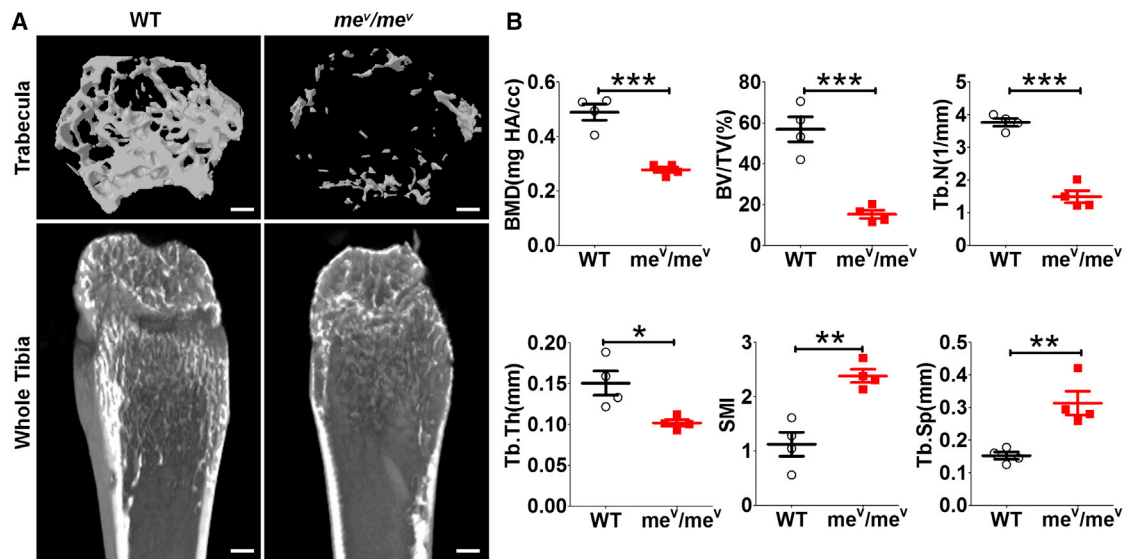


Figure 1. *me^v/me^v* Mice Develop Osteoporosis with Characteristic Reduced Bone Mass and Lower Bone Density

μCT analysis of tibiae from *me^v/me^v* and WT mice (8-week-old males).

(A) Images of trabecular bone of the tibial metaphysis (top) and entire proximal tibia (bottom). Scale bars, 1 mm.

(B) Trabecular bone parameters were quantitated and compared between *me^v/me^v* and WT mice. BMD, bone mineral density; BV/TV, bone-volume/tissue-volume ratio; Tb.N, trabecular number; Tb.Th, trabecular thickness; SMI, structure model index; and Tb.Sp, trabecular separation

Bars represent mean ± SEM (n = 5). *p < 0.05; **p < 0.01; ***p < 0.001.

generated SHP1^{fl/fl}Dermo1-cre mice that induce a targeted deletion of SHP1 specifically in MSCs during mesenchymal condensation, which precedes osteogenesis and adipogenesis (Plutsky et al., 1992). These mice were found to have less bone and more fat tissue as adults, consistent with the phenotype in SHP1-deficient MSCs. Thus, we present compelling evidence that SHP1 plays an important role in regulating the formation of bone mass and adipose tissue by MSCs.

RESULTS

me^v/me^v Mice Exhibit Decreased Bone Mass and Bone Formation

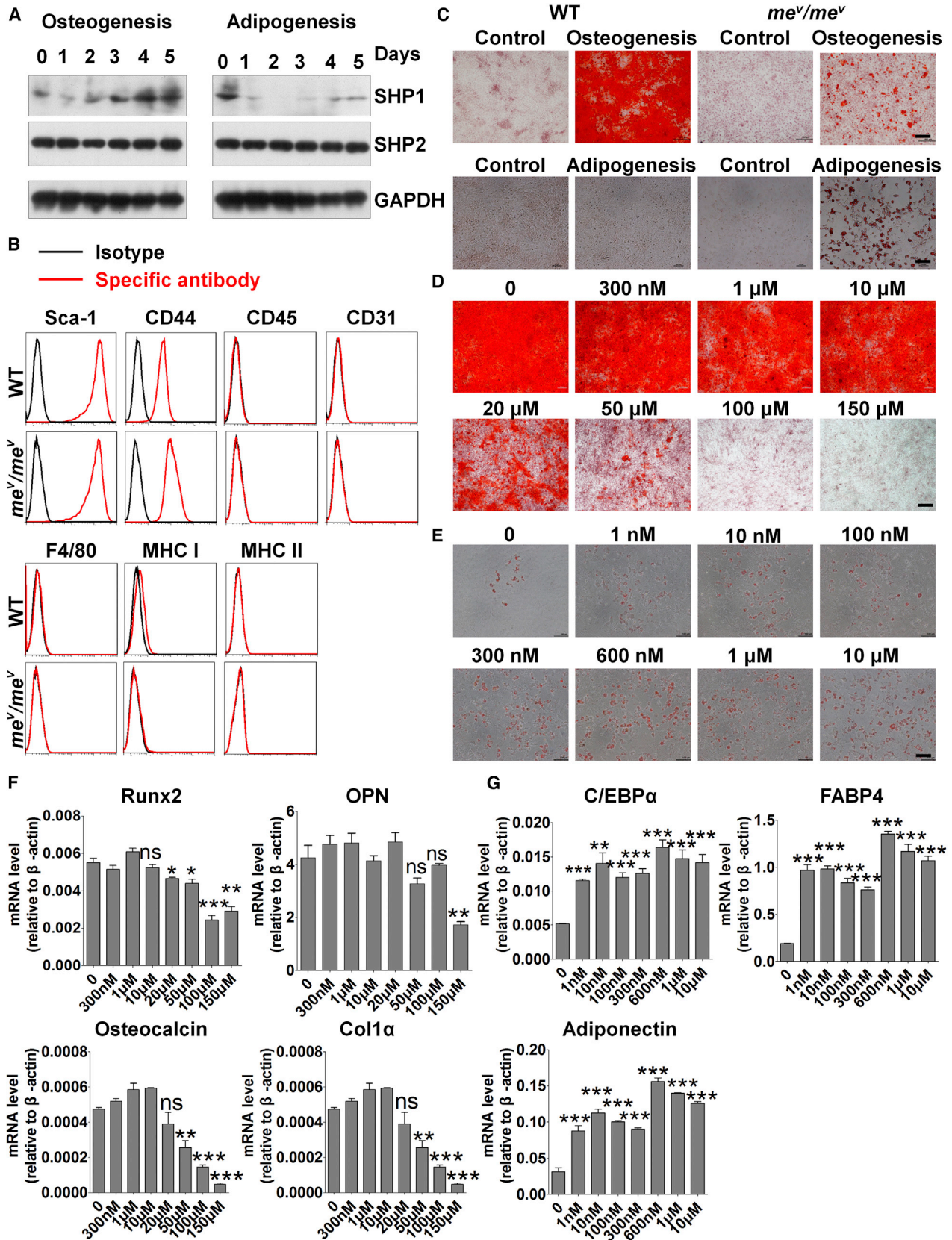
Previous reports have revealed that mice with partial deficiency in SHP1 (*me^v/me^v*) develop spontaneous osteoporosis, including lower bone density and bone thickness relative to WT mice (Aoki et al., 1999). It has also been demonstrated that bone density in the cortex and spongiosa is lower in *me^v/me^v* mice compared with littermate controls (Umeda et al., 1999). To reproduce these previous findings, bones from *me^v/me^v* and WT male mice were analyzed by micro-computed tomography (μCT). μCT analysis of the cortical bone and trabecular bone in the proximal tibia revealed much lower bone mass in *me^v/me^v* mice (Figure 1A). The trabecular bone-volume/tissue-volume ratio (BV/TV) was over 50% lower in the *me^v/me^v* group, compared with WT controls, and was accompanied by 40% lower bone mineral density (BMD), 30% less trabecular thickness (Tb.Th), 60% lower trabecular number (Tb.N), and more than 50% greater trabecular separation (Tb.Sp) (Figure 1B). The structure model index (SMI), which quantifies 3D structure for the relative amounts of plates and rods (SMI = 0, strong bone; SMI = 3, fragile bone), was about

50% higher (Figure 1B). These results indicate that SHP1 influences bone formation in vivo.

me^v/me^v MSCs Promote Less Osteogenesis and More Adipogenesis in an SHP1 Phosphatase-Dependent Manner

The diminished levels of bone formation found in *me^v/me^v* mice led us to hypothesize that SHP1 is involved in osteoblast differentiation. Osteoblasts are a critical component of bone development and maintenance and are known to be derived from MSCs (Heino and Hentunen, 2008). Therefore, we measured protein levels of SHP1 in differentiating MSCs isolated from WT mice, following an established protocol (Ren et al., 2008). Interestingly, SHP1 levels were observed to increase when MSCs were subjected to osteogenic differentiation conditions, while they decreased under adipogenic differentiation conditions (Figure 2A). SHP2, another member of the Src homology phosphatase family that is also known to regulate adipose tissue formation (He et al., 2013), was also measured and found to be expressed at similar levels during both osteogenic and adipogenic differentiation (Figure 2A).

To confirm that SHP1 is involved in the process of MSC differentiation, bone marrow MSCs from *me^v/me^v* and WT mice were monitored during culture for their expression of MSC-specific phenotypic markers (Sung et al., 2008). Immunofluorescence staining followed by flow-cytometric analysis revealed that MSCs from both *me^v/me^v* and WT mice express Sca1 and CD44 at similar levels but do not express CD45, CD31, F4/80, MHC class I, or MHC class II (Figure 2B). Thus, SHP1 had no obvious effect on the MSC phenotype. When MSCs were cultured in either osteogenic or adipogenic differentiation



(legend on next page)

medium, there was a significant difference between me^v/me^v and WT MSCs: as predicted, me^v/me^v MSCs showed diminished osteogenesis and significantly increased adipogenesis compared to WT MSCs (Figure 2C). This suggests that SHP1 plays a key role in controlling the fate of differentiating MSCs in vitro.

Since SHP1, as a protein tyrosine phosphatase, acts by dephosphorylating its target molecules (Zhang et al., 2000), we tested whether this enzymatic activity was involved in SHP1 function during MSC differentiation. When the compound NSC-87877, an inhibitor of SHP1 phosphatase activity, was added during WT MSC differentiation under specific conditions, significantly reduced osteogenesis and enhanced adipogenesis were observed (Figures 2D and 2E), and these effects were found to be dose dependent. The expression profiles of key transcription factors and differentiation markers were analyzed by real-time PCR after MSCs were subjected to specific differentiation conditions. We found that high concentrations of the SHP1 inhibitor resulted in significantly lower levels of Runx2 and associated osteogenic markers, including osteopontin (OPN), collagen 1 α (Col1 α), and osteocalcin (OCN) in the MSCs (Figure 2F). Interestingly, even with low concentrations of SHP1 inhibitor, MSCs displayed strikingly higher levels of C/EBP α and adipogenic markers, including fatty-acid-binding protein 4 (FABP4) and adiponectin (Figure 2G). These results indicate that the phosphatase activity of SHP1 influences MSC differentiation.

SHP1, but Not SHP2, Is Indispensable for the Normal Differentiation of MSCs

Because NSC-87887 is not specific for SHP1, it might also partially inhibit SHP2 activity (Chen et al., 2015). To parse out their effects, SHP1 and SHP2 were individually knocked down in WT MSCs; effective knockdown was achieved for both proteins (Figures 3A and 3D). When SHP1-knockdown MSCs were then cultured in differentiation medium, we found that adipogenic differentiation was favored over osteogenic differentiation. To better quantify this effect, the extent of the differentiated area was calculated using IMT i-Solution software, and differences in the percentage of differentiated areas were found to be highly significant (Figures 3B and 3C). In contrast, SHP2-knockdown MSCs displayed similar amounts of both osteogenesis and adipogenesis and little difference in calculated areas of differentiation (Figures 3E and 3F). To further verify the role of SHP1, MSCs were transfected with a constitutive SHP1 expression cassette,

and SHP1 expression was examined by western blotting (WB) (Figure 3G). When these SHP1-overexpressing MSCs were cultured in the respective differentiation media, we observed enhanced osteogenesis and reduced adipogenesis compared to WT controls. Software analysis of the extent of differentiated area confirmed a significant difference (Figures 3H and 3I). These results indicate that SHP1, but not SHP2, is required for the normal differentiation of MSCs.

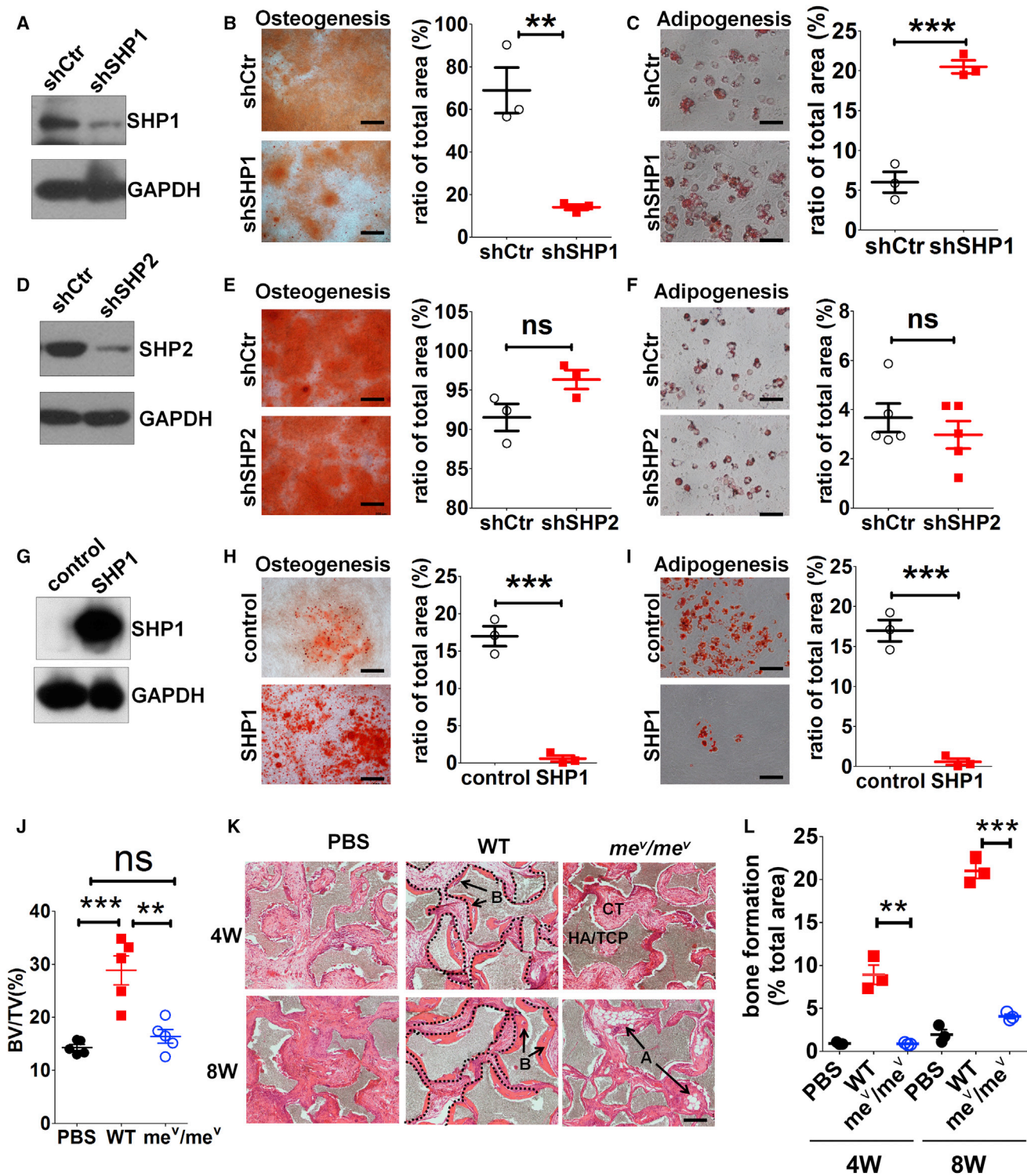
To compare the differentiation capacities in vivo of WT MSCs and me^v/me^v MSCs, an MSC implantation system was used. Carrier particles of hydroxyapatite tricalcium phosphate (HA/TCP) were mixed with MSCs and then implanted subcutaneously under the dorsal skin of nude mice. After 4 or 8 weeks, the implants were harvested and analyzed by micro-CT and H&E staining. Micro-CT analysis revealed a dramatically lower BV/TV in me^v/me^v MSCs, indicating little bone formation on the HA/TCP particles in comparison to WT controls (Figure 3J). Histological analysis revealed consistently that WT MSCs formed more bone than did me^v/me^v MSCs, while me^v/me^v MSCs formed some adipocytes but no bone mass in the HA/TCP particles (Figure 3K). When the areas of bone formation revealed by H&E staining were quantitated using ImageJ software, bone formation was found to be much lower in the me^v/me^v MSC group than in the WT MSC group at 4 or 8 weeks (Figure 3L).

SHP1 Modulates the Expression of Transcription Factors that Regulate Differentiation

Previous studies have shown that Runx2 plays an important role in osteogenic differentiation (Gersbach et al., 2006) and that C/EBP α , C/EBP β , and PPAR γ are key factors driving the adipogenic differentiation of MSCs (Cristancho and Lazar, 2011). Therefore, expression of these transcription factors in WT MSCs and me^v/me^v MSCs was assayed by real-time PCR and WB after up to 9 days in culture. At the mRNA level, me^v/me^v MSCs showed markedly lower levels of Runx2 and osteogenic markers, including OPN, Col1 α , and OCN, in both naive and differentiated states in comparison to WT controls (Figure 4A). In addition, me^v/me^v MSCs displayed higher levels of C/EBP α and adipogenic markers, including FABP4 and adiponectin, than did WT MSCs (Figure 4B). At the protein level, me^v/me^v MSCs had significantly higher levels of C/EBP α and PPAR γ , but less Runx2, than did WT MSCs, even when naive (Figure 4C). However, protein levels of C/EBP β were comparable in WT MSCs and me^v/me^v MSCs (Figure 4C).

Figure 2. SHP1 Deficiency Promotes the Adipogenic, but Not Osteogenic, Differentiation of MSCs

- (A) WT MSCs were cultured in adipogenic or osteogenic differentiation medium for the indicated number of days, and total protein was harvested and subjected to WB to detect SHP1 and SHP2. GAPDH, loading control.
- (B) After isolation from bone marrow of me^v/me^v or WT mice and culture for an equal number of passages, MSCs were harvested, stained for the indicated markers by immunofluorescence, and analyzed by flow cytometry.
- (C) me^v/me^v and WT MSCs were cultured in adipogenic or osteogenic differentiation medium for several days and then stained with alizarin red S to reveal calcium deposition characteristic of osteogenesis or with oil red O to reveal triglycerides representative of adipogenesis. Scale bars, 500 μ m (top) and 100 μ m (bottom).
- (D and E) Graded concentrations of NSC-87877, an SHP1 phosphatase inhibitor, were added to the osteogenic (D) or adipogenic (E) differentiation medium of MSCs cultured as in (C) above, and resultant MSCs were stained with alizarin red S (D) or Oil Red O (E). Scale bars, 500 μ m in (D) and 100 μ m in (E).
- (F) WT MSCs were subjected to osteogenic differentiation in the presence of the inhibitor NSC-87877, and expression levels of Runx2, osteopontin (OPN), collagen 1 α (Col1 α), and osteocalcin (OCN) on the indicated days were analyzed by real-time PCR.
- (G) WT MSCs were subjected to adipogenic differentiation, and C/EBP α , FABP4, and adiponectin were analyzed as in (F).
- Bars represent means \pm SEM. *p < 0.05; **p < 0.01; ***p < 0.001; ns, not significant.



(legend continued on next page)

After SHP1 and SHP2 were individually knocked down in WT MSCs, protein expression was analyzed by WB. We found that SHP1-knockdown MSCs expressed more C/EBP α and PPAR γ , but similar amounts of Runx2 and C/EBP β , in comparison to control MSCs (Figure 4D). In contrast, SHP2-knockdown MSCs exhibited unchanged levels of C/EBP α , C/EBP β , PPAR γ , and Runx2 (Figure 4E). We also found, conversely, that adipogenic transcription factors, including C/EBP α , C/EBP β , and PPAR γ , were decreased in SHP1-overexpressing MSCs, while Runx2 was increased, even under naive conditions (Figure 4F). These results indicate that SHP1 regulates critical transcription factors during MSC differentiation.

Signaling from Wnt, but Not BMP, Is Involved in Impaired Osteogenic Differentiation by SHP1-Deficient MSCs

The Wnt and BMP signaling pathways are well known to play important roles in regulating MSC differentiation (Ling et al., 2009). Wnt signaling through the canonical β -catenin-dependent pathways is considered pro-osteogenic and anti-adipogenic (Case and Rubin, 2010; Glass et al., 2005). To examine whether SHP1 has a regulatory role in Wnt signaling, the expression levels of total β -catenin and non-phospho- β -catenin after treatment with Wnt3a were measured in both *me^v/me^v* MSCs and WT MSCs by WB. We observed that both total β -catenin and non-phospho- β -catenin were dramatically decreased in *me^v/me^v* MSCs compared to WT MSCs (Figure 5A). β -catenin phosphorylation is mediated by GSK3 β , whose activity is regulated by site-specific phosphorylation; full activity of GSK-3 β generally requires phosphorylation at tyrosine 216 (Tyr216); conversely, phosphorylation at serine 9 (Ser9) inhibits GSK-3 β activity. Consistently, we found that GSK3 β phosphorylation at Tyr216 was slightly increased, while phosphorylation at Ser9 was detectably decreased in *me^v/me^v* MSCs, although total protein levels of GSK3 β were no different from those in controls (Figure 5B). This indicates that Wnt signaling is diminished in SHP1-deficient (*me^v/me^v*) MSCs.

To further determine how SHP1 regulates the Wnt signaling pathway, the target molecules of SHP1 had to be defined. To address this, we examined the interaction between SHP1 and GSK3 β in Wnt3a-treated SHP1-overexpressing MSCs using immunoprecipitation and WB. First, the amounts of SHP1 and GSK3 β were determined in whole-protein lysates of SHP1-overexpressing MSCs before and after Wnt3a treatment, normalized to GAPDH levels (Figure 5C). Next, immunoprecipitation with SHP1 revealed that large amounts of GSK3 β coprecipitated with SHP1 in the lysates from SHP1-overexpressing MSCs both before and after Wnt3a treatment. Additional evidence of

the interaction between GSK3 β and SHP1 was provided by GSK3 β immunoprecipitation, which resulted in the coprecipitation of SHP1 (Figure 5C). Additionally, small amounts of β -catenin and non-phospho- β -catenin were detected after SHP1 immunoprecipitation (Figures S1A and S1B). SHP1 binding of β -catenin and non-phospho- β -catenin may result from the binding of β -catenin to GSK3 β . These results indicate that SHP1 regulates the Wnt signaling pathway by forming a complex with GSK3 β that dephosphorylates GSK3 β at Tyr216, thereby inhibiting its enzymatic activity. In turn, β -catenin phosphorylation is decreased, leading to the accumulation and nuclear translocation of β -catenin, thereby activating gene expression (Figure 5D).

We also examined whether SHP1 is involved in the BMP signaling pathway. In this pathway, Smad4 interacts with other phosphorylated Smads to form homomeric or heteromeric complexes, which then translocate to the nucleus, where they regulate the transcription of downstream genes (Li, 2008). When the levels of Smad4 and phosphorylated Smad1/5/9 were measured in MSCs treated with BMP2 or BMP4, no obvious difference was observed between SHP1-deficient and control MSCs (Figures S1C and S1D). Therefore, BMP signaling is unlikely to be involved in the impaired osteogenesis observed in SHP1-deficient MSCs.

Conditional Deletion of SHP1 Interferes with Fat and Bone Formation

We have shown that inactivation of SHP1 in MSCs in vitro and in vivo results in greatly reduced osteogenic differentiation and less bone formation. To further test whether SHP1 plays an important role in bone formation, we utilized the Cre-Lox recombination system to knock out SHP1 in MSCs in vivo. SHP1^{fl/fl} mice were crossed with Dermo1-cre mice, in which cre activity occurs during mesenchymal condensation and later in condensed mesenchyme-derived chondrocytes and osteoblasts (Li et al., 1995). Therefore, we predicted that SHP1^{fl/fl} Dermo1-cre mice would lack SHP1 in mesenchymal progenitor cells. Indeed, we observed shorter teeth in 3-week-old SHP1^{fl/fl} Dermo1-cre mice (Figure 6A). To characterize the osteoblast differentiation defects in SHP1^{fl/fl} Dermo1-cre mice, femurs were analyzed by micro-CT. Insufficient development in the bone of the proximal tibia was observed in SHP1^{fl/fl} Dermo1-cre mice compared with control SHP1^{fl/fl} mice (Figure 6B). In addition, trabecular BV/TV was decreased by more than half, BMD was 20% lower, SMI almost doubled, Tb.Th and Tb.N were less, and Tb.Sp was increased (Figure 6C). Microscopic examination of H&E-stained bone sections showed that fewer trabeculae had developed in SHP1^{fl/fl} Dermo1-cre

(G) WT MSCs were transfected by lentivirus containing an SHP1-expression vector or control vector, and SHP1 expression was measured by WB.

(H and I) SHP1-overexpressing MSCs and control MSCs were cultured in differentiation medium and stained respectively with alizarin red S for osteogenesis or oil red O for adipogenesis. The stained area was quantitated using IMT i-Solution software. Scale bars, 500 μ m in (H) and 100 μ m in (I).

(J) MSCs were mixed with HA/TCP, incubated overnight, and the mixture was implanted subcutaneously under the dorsal skin of nude mice. After 8 weeks, the implants were removed, fixed in 4% paraformaldehyde, and analyzed by micro-CT to determine bone-volume/tissue-volume ratio (BV/TV). PBS, control HA/TCP implanted into nude mice.

(K) Excised implants were paraffin embedded, sectioned, and stained with H&E, and then examined microscopically. Dotted lines delineate the boundary between bone (B) and connective tissues (CT), and the arrowheads indicate areas of bone or adipose (A) formation. HA/TCP, hydroxyapatite tricalcium phosphate. Scale bar, 500 μ m. W, weeks.

(L) Based on H&E staining, the amount of bone that formed on the HA/TCP particles at 4 and 8 weeks was quantitated using ImageJ software.

Bars represent mean \pm SEM (n = 3). **p < 0.01; ***p < 0.001; ns, not significant.

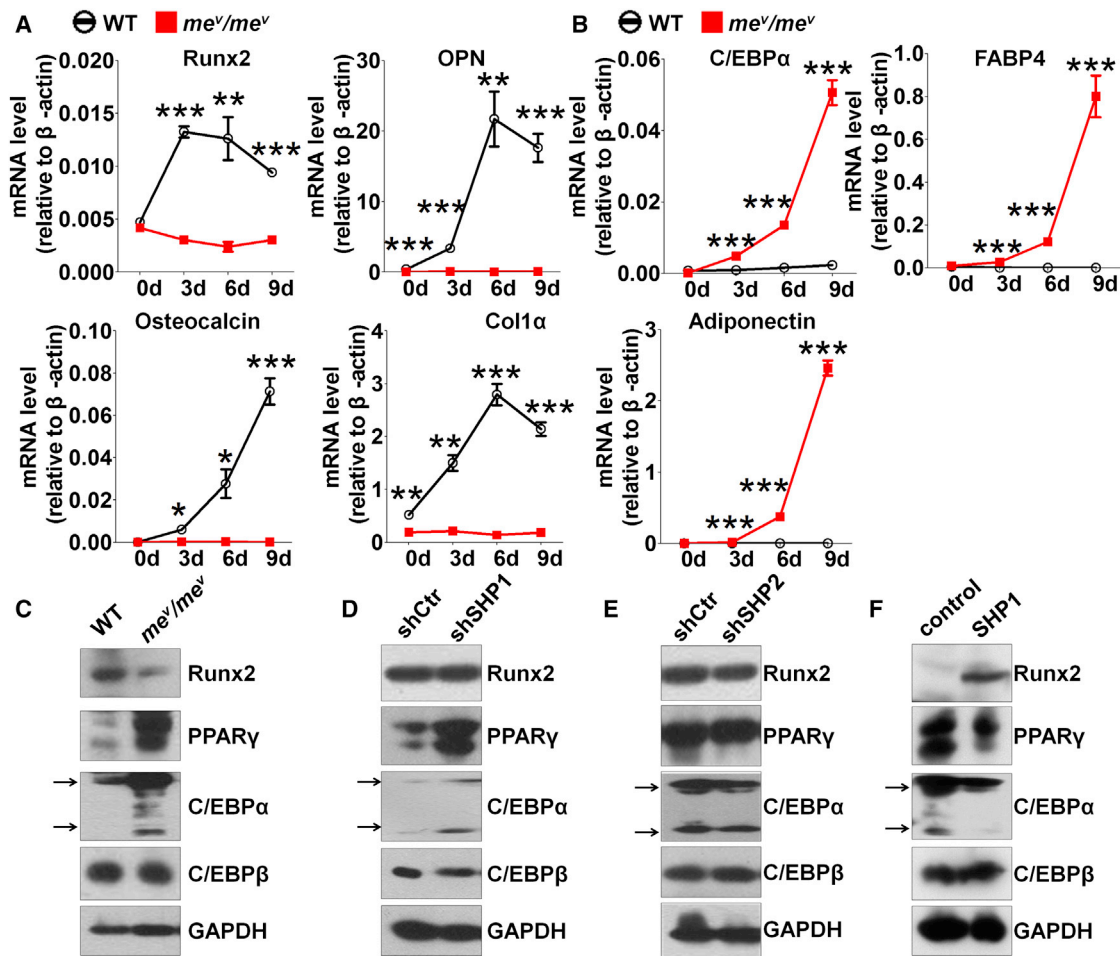


Figure 4. SHP1 Regulates Transcription Factors Critical for MSC Differentiation

(A) WT and *mev/mev* MSCs were subjected to osteogenic differentiation, and expression levels of Runx2, osteopontin (OPN), collagen 1α (Col1α), and osteocalcin (OCN) on indicated days were analyzed by real-time PCR. d, days.

(B) WT and *mev/mev* MSCs were subjected to adipogenic differentiation, and C/EBPα, FABP4, and adiponectin were analyzed, as in (A).

(C) Protein levels of Runx2, PPARγ, C/EBPα, and C/EBPβ were analyzed in naive WT and *mev/mev* MSCs by WB. Arrows indicate 42 knockdown C/EBPα (top) and 28 knockdown C/EBPα (bottom).

(D–F) Naive SHP1-knockdown MSCs (D), SHP2-knockdown MSCs (E), and SHP1-overexpressing MSCs (F), as well as respective controls (Ctrl), were analyzed for expression of Runx2, C/EBPα, C/EBPβ, and PPARγ using WB.

The differences between the means of WT and *mev/mev* MSCs at each time point for three independent biological replicates were compared statistically. Bars represent mean ± SEM (n = 3). *p < 0.05; **p < 0.01; ***p < 0.001.

mice (Figure 6D). Interestingly, however, higher fat-to-body-weight ratios and more gonadal fat tissue deposition occurred under a normal diet in both male and female SHP1^{fl/fl}Dermo1-cre mice, compared to SHP1^{fl/fl} controls, while the amounts of subcutaneous fat tissue were comparable (Figure 6E). The opposite tendencies of subcutaneous and gonadal fat tissue distribution in SHP1^{fl/fl}Dermo1-cre mice could be explained by their different mechanisms of development (Wang et al., 2013, 2015). The fat tissue deposition patterns reveal that SHP1 deletion affects mainly adipocyte differentiation in gonadal fat tissue. Greater fat tissue development in SHP1^{fl/fl}Dermo1-cre mice is consistent with the increased adipogenesis seen in SHP1-deficient MSCs. These results further illustrate that conditional deletion of SHP1 during mesenchymal condensation

delays bone formation, while it enhances gonadal fat tissue formation.

DISCUSSION

Previous reports have demonstrated that systemic SHP1 deficiency in mice induces significant osteoporosis. However, the mechanism has not been conclusively determined, nor is it known whether the observed reduction in osteoblast function is directly related to a lack of SHP1. Here, we have identified SHP1 to be a critical regulator of bone mass that functions by controlling the fate of MSC differentiation, toward either an osteogenic phenotype or an adipogenic one. The effects of SHP1 on MSC differentiation are exerted through its regulation

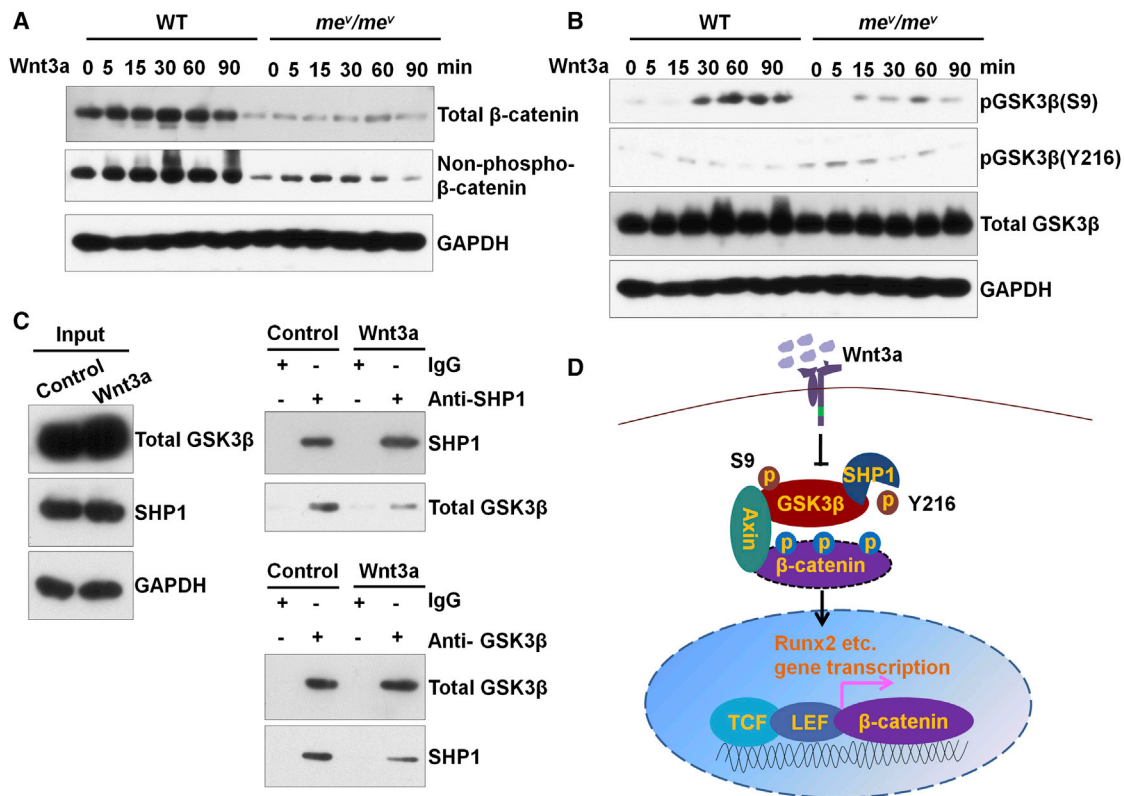


Figure 5. Wnt Signaling Is Upregulated by SHP1 via Dephosphorylation of GSK3 β at Tyr216

(A) WT and *me^v/me^v* MSCs were treated with Wnt3a (20 ng/ml) for the indicated times, and non-phospho- β -catenin and total β -catenin expression levels were evaluated by WB.

(B) WT and *me^v/me^v* MSCs were treated as in (A), and expression of GSK3 β phosphorylated at either Tyr216 (pGSK3 β (Y216)) or at Ser9 (pGSK3 β (S9)) and total GSK3 β were determined.

(C) SHP1-overexpressing MSCs were treated with Wnt3a (20 ng/ml) for 30 min, and cell lysates were analyzed for total GSK3 β and SHP1 by WB (left) or were immunoprecipitated (right) with anti-SHP1 (top) or anti-GSK3 β (bottom).

(D) Diagrammatic representation of the interaction between SHP1, GSK3 β , and other regulatory proteins in Wnt3a signaling (see Discussion for description).

of the expression of lineage-specific transcription factors, including C/EBPs, PPAR γ , and Runx2, and are linked to upregulation of Wnt signaling.

Osteoblasts and adipocytes are both derived from the same MSC precursors. Therefore, the effect of SHP1 deficiency on the differentiation capacity of MSCs was examined in vitro and ex vivo, using cells from SHP1-deficient mice. We found, in vitro, that SHP1-deficient MSCs have enhanced adipogenic differentiation, while osteogenic differentiation is reduced. In addition, the epitomic bone formation assay demonstrated that SHP1 is critical for controlling the differentiation of MSCs. Moreover, adipocyte formation was observed in HA/TCP particles coated with *me^v/me^v* MSCs but not with WT MSCs. The lineage differentiation of MSCs is controlled by several specific transcription factors. Adipogenic differentiation is dependent on the C/EBP family and PPAR γ (Tontonoz et al., 1994), whereas osteogenic differentiation requires chiefly Runx2 (Ducy et al., 1997). When expression of these pivotal transcription factors during MSC differentiation was analyzed by WB and real-time PCR, the adipogenic transcription factors C/EBP α and PPAR γ were found to be notably

increased in SHP1-deficient MSCs at both the protein and mRNA levels.

The expression and activation of specific transcription factors during MSC differentiation are regulated by several signaling pathways, the most important being Wnt and BMP signaling. Most reports have shown that both of these signaling pathways promote osteogenic differentiation and inhibit adipogenic differentiation. BMP signals control MSC differentiation, mainly by regulating Runx2 expression through the canonical Smad-dependent pathways and non-canonical Smad-independent pathways. BMP family members, such as BMP2, BMP4, and BMP6, have been shown to induce MSC differentiation (Chen et al., 2012). Deletion of BMP2 or BMP4 in mice leads to defects in skeletogenesis and a loss of osteogenesis (Bandyopadhyay et al., 2006). In the present study, however, BMP signals were found to be unaffected by SHP1. The influences of the canonical Wnt/ β -catenin signaling pathway on osteogenic differentiation by MSCs are complex and not yet fully elucidated. For the most part, however, canonical Wnt/ β -catenin signaling is believed to favor osteogenic differentiation by MSCs, rather than adipogenesis, through inhibition of C/EBP and PPAR γ

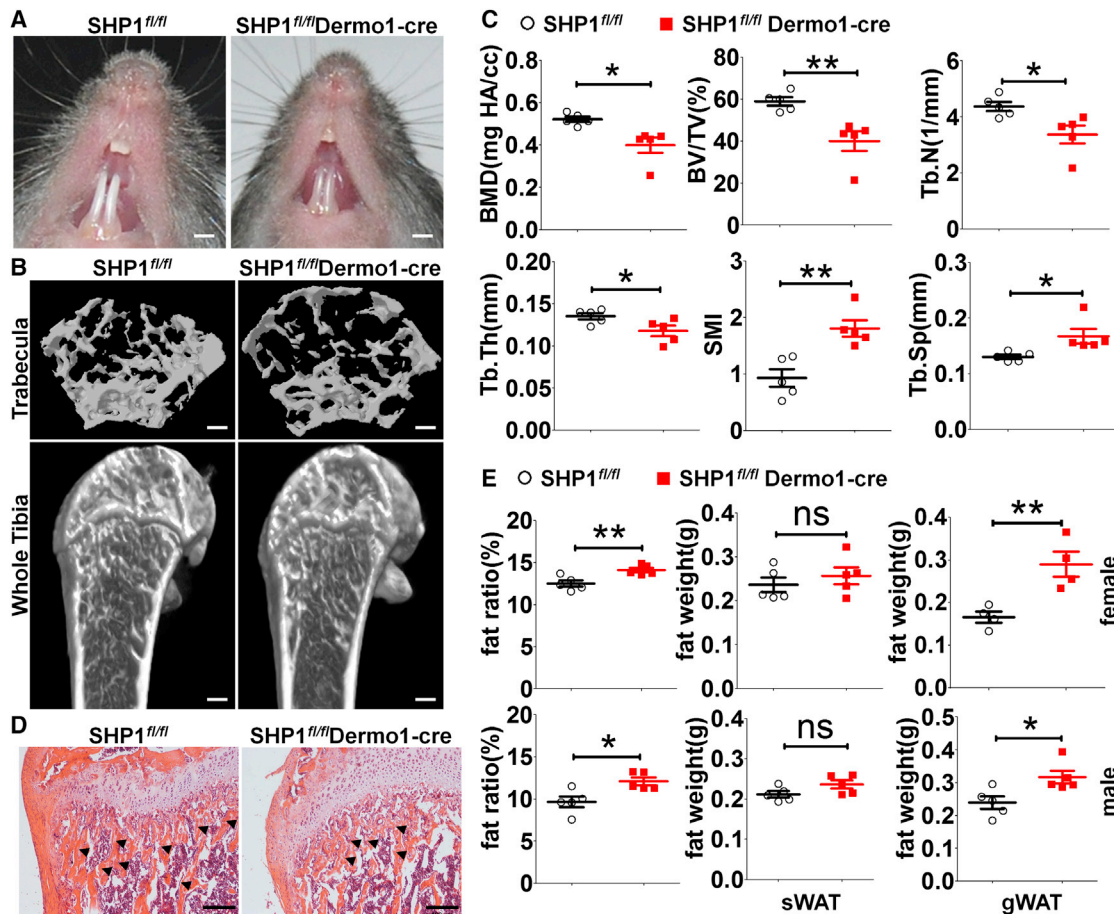


Figure 6. Conditional Deletion of SHP1 Interferes with Fat and Bone Tissue Formation in Mice

Bone formation indicators were compared between SHP1^{fl/fl}Dermo1-Cre mice and SHP1^{fl/fl} controls.

(A) Differences in tooth length at 3 weeks of age. Scale bars, 5 mm.

(B) μ CT images of tibiae from 2-month-old males (representative of five mice) show trabecular bone of the tibial metaphysis (top) and the entire proximal tibia (bottom). Scale bars, 1 mm.

(C) μ CT analysis of tibiae from 2-month-old males (n = 5) revealed differences in trabecular bone parameters: BMD, bone mineral density; BV/TV, bone-volume/tissue-volume ratio; Tb.N, trabecular number; Tb.Th, trabecular thickness; SMI, structure model index; Tb.Sp, trabecular separation.

(D) Bone was isolated, sectioned, stained with H&E, and observed microscopically. Arrows indicate the developed trabeculae. Scale bars, 500 μ m.

(E) Subcutaneous and gonadal fat tissues were isolated from 2-month-old females (top) or males (bottom) (n = 5) and analyzed for total fat ratio and subcutaneous and gonadal fat weights. sWAT, subcutaneous white adipose tissue; gWAT, gonadal white adipose tissue.

Bars represent mean \pm SEM (n = 5); ns, not significant; *p < 0.05; **p < 0.01.

expression. For instance, Wnt receptor ligands, such as Wnt6, Wnt10a, and Wnt10b, are reported to promote osteogenic MSC differentiation through canonical β -catenin signaling (Baksh and Tuan, 2007). Studies in which Wnt10b gene dosages were altered have revealed that Wnt10b is a positive regulator of bone formation, as it enhances osteoblast differentiation, and it maintains mesenchymal progenitors, osteoblast progenitors, or both in adult bone (Bennett et al., 2007; Stevens et al., 2010).

Protein phosphorylation and dephosphorylation at tyrosyl residues are important regulatory mechanisms that modulate the activity of proteins involved in the process of cell growth and differentiation. SHP1 acts as both a positive and a negative regulator of signal transduction. SHP1 was previously shown to significantly reduce β -catenin/TCF-dependent transcription

in intestinal crypt epithelial cells by binding to and dephosphorylating β -catenin (Duchesne et al., 2003). SHP1 has also been demonstrated to interfere with β -catenin activity by promoting its degradation in a GSK3 β -dependent manner (Simoneau et al., 2011). Therefore, to verify the role of SHP1, we analyzed Wnt/ β -catenin signaling in SHP1-deficient MSCs derived from *me^v/me^v* mice. When treated with Wnt3a, *me^v/me^v* MSCs displayed remarkably less non-phospho- β -catenin and more GSK3 β phosphorylation at Tyr216, each of which is involved in the Wnt signaling pathway. In addition, GSK3 β phosphorylation at Ser9, which is mediated by AKT, was decreased in *me^v/me^v* MSCs, the cause of which remains to be determined. GSK3 β is negatively regulated by PI3K (phosphatidylinositol 3-kinase)-mediated activation of AKT/PKB (protein kinase B) and by the

WNT signaling pathway (Clodfelder-Miller et al., 2005). In the absence of Wnt signals, the scaffolding protein AXIN (Axis inhibitor) helps GSK3 β to efficiently bind to and phosphorylate β -catenin, thus targeting it for ubiquitination and subsequent proteosomal degradation. SHP1 has two tandem SH2 domains at the N terminus: a single central catalytic domain and a C-terminal domain. The SH2 domains recruit SHP1 to tyrosine-phosphorylated molecules, enabling dephosphorylation to be performed by the catalytic domain. Using SHP1 immunoprecipitation in SHP1-overexpressing MSCs, we revealed that SHP1 binds to GSK3 β . Therefore, we propose that SHP1 regulates Wnt/ β -catenin signaling by binding to and dephosphorylating GSK3 β at the Tyr216 site. Since dephosphorylation inactivates GSK3 β , thereby preventing β -catenin phosphorylation, β -catenin is allowed to accumulate and to translocate to the nucleus, where it upregulates transcription factor expression.

Both *me/me* mice and *me^v/me^v* mice display bone loss phenotypes. The development, growth, and repair of the skeletal system involve complex processes that are mediated by multiple cell lineages, including osteoblasts, osteoclasts, and chondrocytes. In order to further investigate the function of SHP1 in the skeletal system, we used a conditional gene deletion approach, utilizing the Cre-LoxP system to generate SHP1^{fl/fl}Dermo1-cre mice. Since Dermo1 is expressed during mesenchymal condensation, which was confirmed by lineage tracing analysis after crossing with the R26R mouse (Soriano, 1999), SHP1 is deleted in progenitor MSCs that can generate both osteoblast and chondrocyte lineage cells. This analysis also showed that both osteoblasts and chondrocytes, derived from condensed mesenchyme, did indeed express Dermo1-cre (Liu et al., 2010). In addition, Dermo1-cre has been shown to be specifically expressed in bone marrow-derived MSCs (Liu et al., 2010). Significantly, SHP1^{fl/fl} Dermo1-cre mice showed characteristics of osteoporosis, including fewer trabeculae and shorter teeth, because of insufficient osteoblast formation. In addition, the amount of adipose tissue in the gonads was increased. These results further illustrate that SHP1 deficiency in MSCs leads to abnormalities in bone formation.

In conclusion, this study suggests that SHP1 regulates bone and fat development in adults by influencing the balance between osteoblast differentiation and adipocyte differentiation by MSCs. The tendency toward adipogenic differentiation appears to be favored in the absence of normal SHP1, suggesting that SHP1 is a positive regulator of osteogenesis and a negative regulator of adipogenesis.

EXPERIMENTAL PROCEDURES

Mice Generation and Maintenance

Dermo1-cre mice and *me^v/me^v* mice (C57BL/6J background) were purchased from the Jackson Laboratory. SHP1^{fl/fl} mice were kindly supplied by the lab of W.X. in the Second Military Medical University. Dermo1-cre mice were mated with SHP1^{fl/fl} mice for at least three generations to generate SHP1^{fl/fl} Dermo1-cre mice. Female immunocompromised nude mice (BALB/c, nu/nu) were purchased from the SLAC (Shanghai Laboratory Animal Center) of the Chinese Academy of Sciences. All procedures were approved by the Institutional Animal Care and Use Committee of the Institute of Health Sciences, Shanghai Institutes for Biological Sciences of the Chinese Academy of Sciences.

Cell Culture

Using our lab-developed protocol, the tibias and femurs of 6- to 10-week-old WT and age-matched *me^v/me^v* mice were dissected from the surrounding tissues, the bones were cut, and bone marrow cells were collected by flushing with low-glucose DMEM (Invitrogen). Cell cultures were incubated in a humidified environment containing 5% CO₂ at 37°C.

Reagents

Reagents for inducing MSC differentiation, including indomethacin, dexamethasone, insulin, 3-isobutyl-1-methylxanthine, L-ascorbic acids, and β -glycerophosphate, as well as alizarin red S, oil red O, and formaldehyde solution were purchased from Sigma-Aldrich. Antibodies used in WB were: SHP1 (Abcam); Runx2 (Epitomics); C/EBP α , C/EBP β , PPAR γ , β -catenin, GSK3 β , non-phospho- β -catenin, pGSK3 β , and GAPDH (Cell Signaling Technology).

Differentiation of MSCs

Accordingly, to induce osteogenic differentiation, MSCs were cultured in high-glucose DMEM supplemented with 10% heat-inactivated FBS, 10 nM dexamethasone, 100 mM L-ascorbic acid, and 10 mM β -glycerophosphate. Adipogenic differentiation was induced with high-glucose DMEM containing 0.5 mM isobutylmethylxanthin, 60 mM indomethacin, 100 nM dexamethasone, and 10 mg/ml insulin.

Histological Analysis of Differentiated BMSC Cultures

Osteogenesis was evaluated by alizarin red S staining. In brief, the cells were fixed in cold 70% ethanol for 1 hr, washed twice with H₂O, and incubated with 2% alizarin red S (pH = 4.1 to 4.3) for about 15 min to reveal calcium deposition. Adipogenesis was assessed by oil red O staining to reveal triglycerides: the cells were fixed in 10% formalin for 1 hr, washed twice with H₂O, allowed to air dry, and then stained with oil red O for about 30 min at room temperature.

Ectopic Bone Formation

Bone-marrow-derived MSCs (2×10^5) were mixed overnight with carrier particles of ceramic HA-TCP (40 mg; Bio-lu Biomaterials Company), and this mixture was implanted subcutaneously under the dorsal skin of nude mice. After 4 or 8 weeks, mice were euthanized, and the harvested particles were fixed in 4% paraformaldehyde overnight. The particles were analyzed by μ CT and stained with H&E and embedded in paraffin for preparing thin sections.

Lentivirus Transfection

The lentivirus particles for knocking down SHP1 protein were purchased from GeneChem. MSCs were infected with the described lentiviral vectors in low-glucose DMEM supplemented with 10 mg/ml polybrene (GeneChem). After transfection, MSCs were selected in medium containing puromycin.

Flow-Cytometric Analysis

Cells were harvested after trypsinization and stained with fluorophore-conjugated antibodies for 30 min on ice. The cell samples were analyzed using a BD FACSCalibur flow cytometer (BD Biosciences). FlowJo software was used for data analysis.

WB

MSCs were scraped off the culture surface and lysed using RIPA lysis buffer (BeyoTime) on ice. Total protein concentration was measured with the BCA protein assay kit (Bio-Rad). Protein samples were separated by SDS-PAGE and transferred to a nitrocellulose membrane, which was then blocked with 5% fat-free milk. Blots were incubated with specific primary antibodies followed by anti-rabbit-HRP (horseradish peroxidase), and staining was detected with the ECL system (Millipore).

Real-Time PCR

Total RNA was extracted using TRIzol (Invitrogen). First-strand cDNA was synthesized using the cDNA Synthesizing Kit (Takara) according to the manufacturer's instructions. cDNA was applied as a template to determine the expression of specific genes in real-time PCR with SYBR Green reagent from Takara. Gene expression was normalized to endogenous β -actin mRNA.

Statistical Analysis

Statistical analysis was performed using Prism 5.0 software (GraphPad). Unpaired two-tailed Student's *t* test was used in all instances, and statistical significance is reported as follows: ns, not significant; **p* < 0.05; ***p* < 0.01; ****p* < 0.001. Bars represent means ± SEM.

SUPPLEMENTAL INFORMATION

Supplemental Information includes one figure and can be found with this article online at <http://dx.doi.org/10.1016/j.celrep.2016.06.035>.

AUTHOR CONTRIBUTIONS

M.J.: conception and design, collection and assembly of data, data analysis and interpretation, manuscript writing; C.Z.: collection and/or assembly of data, data analysis and interpretation; P.S.: collection and/or assembly of data, data analysis and interpretation; N.L.: lentivirus preparation, data analysis and interpretation; G.C.: data analysis and interpretation, manuscript writing; Q.C.: data analysis and interpretation; C.X.: lentivirus preparation, data analysis and interpretation; L.D.: data analysis and interpretation; Q.Y.: data analysis and interpretation; J.C.: data analysis and interpretation; Y.H.: tissue sectioning and H&E staining; F. Li: mouse breeding and genotyping; W.C.: conception and design, data analysis and interpretation; F. Liu: conception and design, data analysis and interpretation; A.B.R.: manuscript writing; A.I.R.: manuscript writing; W.X.: provided mice; Y.W.: conception and design, data analysis and interpretation, manuscript writing; Y.S.: conception and design, data analysis and interpretation, financial support, manuscript writing, final approval of manuscript.

ACKNOWLEDGMENTS

We thank Dr. Douglas Green for comments and suggestions. This study was supported by grants from the Scientific Innovation Project of the Chinese Academy of Science (XDA 01040100); the Ministry of Science and Technology of China (2015CB964400), the Programs of National Natural Science of China (81330046, 81273316, 81571612, 81530043, 31571404 and 31401168); the External Cooperation Program of BIC, Chinese Academy of Sciences (GJHZ201307); the Shanghai Rising-Star Program (14QA1404200); and the Youth Innovation Promotion Association, Chinese Academy of Sciences.

Received: December 30, 2015

Revised: April 3, 2016

Accepted: June 5, 2016

Published: July 7, 2016

REFERENCES

Aoki, K., Didomenico, E., Sims, N.A., Mukhopadhyay, K., Neff, L., Houghton, A., Amling, M., Levy, J.B., Horne, W.C., and Baron, R. (1999). The tyrosine phosphatase SHP-1 is a negative regulator of osteoclastogenesis and osteoclast resorbing activity: increased resorption and osteopenia in *me(v)/me(v)* mutant mice. *Bone* 25, 261–267.

Baksh, D., and Tuan, R.S. (2007). Canonical and non-canonical Wnts differentially affect the development potential of primary isolate of human bone marrow mesenchymal stem cells. *J. Cell. Physiol.* 212, 817–826.

Bandyopadhyay, A., Tsuji, K., Cox, K., Harfe, B.D., Rosen, V., and Tabin, C.J. (2006). Genetic analysis of the roles of BMP2, BMP4, and BMP7 in limb patterning and skeletogenesis. *PLoS Genet.* 2, e216.

Bennett, C.N., Longo, K.A., Wright, W.S., Suva, L.J., Lane, T.F., Hankenson, K.D., and MacDougald, O.A. (2005). Regulation of osteoblastogenesis and bone mass by Wnt10b. *Proc. Natl. Acad. Sci. USA* 102, 3324–3329.

Bennett, C.N., Ouyang, H., Ma, Y.L., Zeng, Q., Gerin, I., Sousa, K.M., Lane, T.F., Krishnan, V., Hankenson, K.D., and MacDougald, O.A. (2007). Wnt10b increases postnatal bone formation by enhancing osteoblast differentiation. *J. Bone Miner. Res.* 22, 1924–1932.

Case, N., and Rubin, J. (2010). Beta-catenin—a supporting role in the skeleton. *J. Cell. Biochem.* 110, 545–553.

Cha, Y., Moon, B.H., Lee, M.O., Ahn, H.J., Lee, H.J., Lee, K.A., Fornace, A.J., Jr., Kim, K.S., Cha, H.J., and Park, K.S. (2010). Zap70 functions to maintain stemness of mouse embryonic stem cells by negatively regulating Jak1/Stat3/c-Myc signaling. *Stem Cells* 28, 1476–1486.

Chamberlain, G., Fox, J., Ashton, B., and Middleton, J. (2007). Concise review: mesenchymal stem cells: their phenotype, differentiation capacity, immunological features, and potential for homing. *Stem Cells* 25, 2739–2749.

Chen, G., Deng, C., and Li, Y.P. (2012). TGF- β and BMP signaling in osteoblast differentiation and bone formation. *Int. J. Biol. Sci.* 8, 272–288.

Chen, C., Cao, M., Zhu, S., Wang, C., Liang, F., Yan, L., and Luo, D. (2015). Discovery of a novel inhibitor of the protein tyrosine phosphatase Shp2. *Sci. Rep.* 5, 17626.

Clodfelder-Miller, B., De Sarno, P., Zmijewska, A.A., Song, L., and Jope, R.S. (2005). Physiological and pathological changes in glucose regulate brain Akt and glycogen synthase kinase-3. *J. Biol. Chem.* 280, 39723–39731.

Cristancho, A.G., and Lazar, M.A. (2011). Forming functional fat: a growing understanding of adipocyte differentiation. *Nat. Rev. Mol. Cell Biol.* 12, 722–734.

Darlington, G.J., Ross, S.E., and MacDougald, O.A. (1998). The role of C/EBP genes in adipocyte differentiation. *J. Biol. Chem.* 273, 30057–30060.

Duchesne, C., Charland, S., Asselin, C., Nahmias, C., and Rivard, N. (2003). Negative regulation of beta-catenin signaling by tyrosine phosphatase SHP-1 in intestinal epithelial cells. *J. Biol. Chem.* 278, 14274–14283.

Ducy, P., Zhang, R., Geoffroy, V., Ridall, A.L., and Karsenty, G. (1997). *Osf2/Cbfa1*: a transcriptional activator of osteoblast differentiation. *Cell* 89, 747–754.

Gersbach, C.A., Le Doux, J.M., Guldberg, R.E., and García, A.J. (2006). Inducible regulation of Runx2-stimulated osteogenesis. *Gene Ther.* 13, 873–882.

Glass, D.A., 2nd, Bialek, P., Ahn, J.D., Starbuck, M., Patel, M.S., Clevers, H., Taketo, M.M., Long, F., McMahon, A.P., Lang, R.A., and Karsenty, G. (2005). Canonical Wnt signaling in differentiated osteoblasts controls osteoclast differentiation. *Dev. Cell* 8, 751–764.

Green, M.C., and Shultz, L.D. (1975). *Motheaten*, an immunodeficient mutant of the mouse. I. Genetics and pathology. *J. Hered.* 66, 250–258.

He, Z., Zhu, H.H., Bauler, T.J., Wang, J., Ciaraldi, T., Alderson, N., Li, S., Raquil, M.A., Ji, K., Wang, S., et al. (2013). Nonreceptor tyrosine phosphatase Shp2 promotes adipogenesis through inhibition of p38 MAP kinase. *Proc. Natl. Acad. Sci. USA* 110, E79–E88.

Heino, T.J., and Hentunen, T.A. (2008). Differentiation of osteoblasts and osteocytes from mesenchymal stem cells. *Curr. Stem Cell Res. Ther.* 3, 131–145.

James, A.W., Pang, S., Askarinam, A., Corselli, M., Zara, J.N., Goyal, R., Chang, L., Pan, A., Shen, J., Yuan, W., et al. (2012). Additive effects of sonic hedgehog and Nell-1 signaling in osteogenic versus adipogenic differentiation of human adipose-derived stromal cells. *Stem Cells Dev.* 21, 2170–2178.

Li, B. (2008). Bone morphogenetic protein-Smad pathway as drug targets for osteoporosis and cancer therapy. *Endocr. Metab. Immune Disord. Drug Targets* 8, 208–219.

Li, L., Cserjesi, P., and Olson, E.N. (1995). *Dermo-1*: a novel twist-related bHLH protein expressed in the developing dermis. *Dev. Biol.* 172, 280–292.

Ling, L., Nurcombe, V., and Cool, S.M. (2009). Wnt signaling controls the fate of mesenchymal stem cells. *Gene* 433, 1–7.

Liu, Y., Wang, L., Fatahi, R., Kronenberg, M., Kalajzic, I., Rowe, D., Li, Y., and Maye, P. (2010). Isolation of murine bone marrow derived mesenchymal stem cells using Twist2 Cre transgenic mice. *Bone* 47, 916–925.

Mizuno, K., Katagiri, T., Maruyama, E., Hasegawa, K., Ogimoto, M., and Yakura, H. (1997). SHP-1 is involved in neuronal differentiation of P19 embryonic carcinoma cells. *FEBS Lett.* 417, 6–12.

Moroni, L., and Fornasari, P.M. (2013). Human mesenchymal stem cells: a bank perspective on the isolation, characterization and potential of alternative sources for the regeneration of musculoskeletal tissues. *J. Cell. Physiol.* 228, 680–687.

- Neve, A., Corrado, A., and Cantatore, F.P. (2011). Osteoblast physiology in normal and pathological conditions. *Cell Tissue Res.* **343**, 289–302.
- Pei, L., and Tontonoz, P. (2004). Fat's loss is bone's gain. *J. Clin. Invest.* **113**, 805–806.
- Pittenger, M.F., Mackay, A.M., Beck, S.C., Jaiswal, R.K., Douglas, R., Mosca, J.D., Moorman, M.A., Simonetti, D.W., Craig, S., and Marshak, D.R. (1999). Multilineage potential of adult human mesenchymal stem cells. *Science* **284**, 143–147.
- Plutzky, J., Neel, B.G., and Rosenberg, R.D. (1992). Isolation of a src homology 2-containing tyrosine phosphatase. *Proc. Natl. Acad. Sci. USA* **89**, 1123–1127.
- Ren, G., Zhang, L., Zhao, X., Xu, G., Zhang, Y., Roberts, A.I., Zhao, R.C., and Shi, Y. (2008). Mesenchymal stem cell-mediated immunosuppression occurs via concerted action of chemokines and nitric oxide. *Cell Stem Cell* **2**, 141–150.
- Shultz, L.D., Rajan, T.V., and Greiner, D.L. (1997). Severe defects in immunity and hematopoiesis caused by SHP-1 protein-tyrosine-phosphatase deficiency. *Trends Biotechnol.* **15**, 302–307.
- Simoneau, M., Coulombe, G., Vandal, G., Vézina, A., and Rivard, N. (2011). SHP-1 inhibits β -catenin function by inducing its degradation and interfering with its association with TATA-binding protein. *Cell. Signal.* **23**, 269–279.
- Soriano, P. (1999). Generalized lacZ expression with the ROSA26 Cre reporter strain. *Nat. Genet.* **21**, 70–71.
- Stevens, J.R., Miranda-Carboni, G.A., Singer, M.A., Brugger, S.M., Lyons, K.M., and Lane, T.F. (2010). Wnt10b deficiency results in age-dependent loss of bone mass and progressive reduction of mesenchymal progenitor cells. *J. Bone Miner. Res.* **25**, 2138–2147.
- Sung, J.H., Yang, H.M., Park, J.B., Choi, G.S., Joh, J.W., Kwon, C.H., Chun, J.M., Lee, S.K., and Kim, S.J. (2008). Isolation and characterization of mouse mesenchymal stem cells. *Transplant. Proc.* **40**, 2649–2654.
- Tontonoz, P., Hu, E., Graves, R.A., Budavari, A.I., and Spiegelman, B.M. (1994). mPPAR gamma 2: tissue-specific regulator of an adipocyte enhancer. *Genes Dev.* **8**, 1224–1234.
- Uccelli, A., Moretta, L., and Pistoia, V. (2008). Mesenchymal stem cells in health and disease. *Nat. Rev. Immunol.* **8**, 726–736.
- Umeda, S., Beamer, W.G., Takagi, K., Naito, M., Hayashi, S., Yonemitsu, H., Yi, T., and Shultz, L.D. (1999). Deficiency of SHP-1 protein-tyrosine phosphatase activity results in heightened osteoclast function and decreased bone density. *Am. J. Pathol.* **155**, 223–233.
- Wang, Q.A., Tao, C., Gupta, R.K., and Scherer, P.E. (2013). Tracking adipogenesis during white adipose tissue development, expansion and regeneration. *Nat. Med.* **19**, 1338–1344.
- Wang, Q.A., Tao, C., Jiang, L., Shao, M., Ye, R., Zhu, Y., Gordillo, R., Ali, A., Lian, Y., Holland, W.L., et al. (2015). Distinct regulatory mechanisms governing embryonic versus adult adipocyte maturation. *Nat. Cell Biol.* **17**, 1099–1111.
- Wu, L., Cai, X., Zhang, S., Karperien, M., and Lin, Y. (2013). Regeneration of articular cartilage by adipose tissue derived mesenchymal stem cells: perspectives from stem cell biology and molecular medicine. *J. Cell. Physiol.* **228**, 938–944.
- Zhang, J., Somani, A.K., and Siminovitch, K.A. (2000). Roles of the SHP-1 tyrosine phosphatase in the negative regulation of cell signalling. *Semin. Immunol.* **12**, 361–378.
- Zhang, L., Su, P., Xu, C., Chen, C., Liang, A., Du, K., Peng, Y., and Huang, D. (2010). Melatonin inhibits adipogenesis and enhances osteogenesis of human mesenchymal stem cells by suppressing PPAR γ expression and enhancing Runx2 expression. *J. Pineal Res.* **49**, 364–372.